ACEPT-AIR

LIFE+ 09 ENV/GR/000289

Action 2

Deliverable D7.

TITLE: PM_{10} and $PM_{2.5}$ Chemical Composition Databases for the three urban areas AMA, TMA and VGA

April 2013

Coordinated by:

Aristotle University of Thessaloniki

Deliverable D7. PM_{10} and $PM_{2.5}$ Chemical Composition Databases for the three urban areas AMA, TMA and VGA

EXECUTIVE SUMMARY

A PM chemical components database was constructed in the framework of the LIFE09 ENV/GR/000289 project "Development of a Cost Efficient Policy Tool for reduction of Particulate Matter in AIR (ACEPT-AIR)" for three urban areas of Greece: the Athens Metropolitan Area (AMA), the Thessaloniki Metropolitan Area (TMA) and the Volos Greater Area (VGA). The database provides the concentrations of major and trace chemical components associated to the particle fractions PM_{10} and $PM_{2.5}$ that were measured during the ACEPT-AIR project, as well as relevant historical data. In particular the the database provides information for: elemental components (major and trace elements including heavy metals), ionic components (SO_4^{-2}, NO_3^-, NH_4^+, Cl^-, Na^+, K^+, Ca^{2+}, Mg^{2+}), carbonaceous species (OC and EC), organic compounds (PAHs, PCBs, OCPs, n-alkanes, etc).

Regarding the carbonaceous species OC and EC, concentrations at both Athens sites and at Volos and Thessaloniki background site were relatively low during the warm period. The low EC/OC ratios at the background sites indicate relatively low contribution from traffic emissions, coupled with secondary organic formation. At the traffic site in Thessaloniki, concentrations were significantly high, among the highest values reported for other urban sites in European cities. Cold period data presented a similar pattern, with OC concentrations contributing the most to total carbon at all sites. The effect of residential heating during this period was apparent in the much higher OC and EC concentrations. The low values of EC/OC concentration ratios during cold season are indicative of biomass burning aerosol and suggest intense use of fireplaces during this season.

At the AMA sites, SO_4^{-2}, NO_3^-, NH_4^+ and Ca^{2+} were the prevalent ions in the PM_{10} fraction *vs.* SO_4^{-2}, NO_3^-, NH_4^+ in the $PM_{2.5}$ fraction. Cl^-, Na^+ and Ca^{2+} exhibited the lowest $PM_{2.5}/PM_{10}$ ratios. $PM_{2.5}/PM_{10}$ ratio values close to 1 were found for $SO_4^{2-}$and NH_4^+at both sites. Similarly, at the TMA sites, SO_4^{-2}, NO_3^-, NH_4^+ and Ca^{2+} were the major ions in the PM_{10} fraction vs SO_4^{-2}, NO_3^-, NH_4^+ in the $PM_{2.5}$ fraction. NO_3^-, Cl^- and Ca^{2+} associated to $PM_{2.5}$ were slightly higher at the UT site, whereas SO_4^{2-} slightly higher at the UB site. The highest $PM_{2.5}/PM_{10}$ ratios were found for NH_4^+ (1.46-1.90), while Ca^{2+} exhibited the lowest $PM_{2.5}/PM_{10}$ ratios (0.16-0.22). Among all sampling sites, Volos presented the highest concentrations for SO_4^{-2}, NH_4^+, K^+, Cl^-, Ca^{2+} in PM_{10}, and the highest concentrations for Na^+, K^+, Ca^{2+} and SO_4^{-2} in $PM_{2.5}$.

At all sites, crustal elements, such as Ca, Si, Fe, Al were the most abundant elemental components in PM_{10} followed by elements related to anthropogenic processes (K, S and Zn). S, K and Ca were the prevalent elements in $PM_{2.5}$. Ca was found in

predominantly high concentrations, particularly at TMA-UT and VGA, where the Ca/Si ratio was highest (4.1 and 3, respectively) suggesting influence from construction sites and road works. Volos among all sampling sites presented the highest concentrations for anthropogenic elements such as Zn, S, K, As, Br, and Pb in PM_{10}, as well as the highest concentrations for K, Ca, Fe, Cu, Zn, Pb, Mg, Al, Si, S, Cl, Mn and As in $PM_{2.5.}$

For the purposes of mass closure, the chemical components were divided into six classes as follows: minerals, trace elements, organic matter (OM), elemental carbon (EC), sea salt and secondary inorganic aerosol (SECONDARY). Secondary aerosol, OM, and minerals dominated the PM_{10} profiles for all sites, while secondary aerosol and OM were by far the prevalent components in $PM_{2.5}$. A significant contribution for EC was apparent at the traffic site TMA-UT reaching 22% in summer time $PM_{2.5}$ mass. Unidentified mass (UN) ranged between 4%-17% in AMA, 13%-32% in TMA and 1%-37% in VGA.

ΠΕΡΙΛΗΨΗ

Μία βάση δεδομένων χημικών συστατικών ΑΣ (Αιωρούμενων Σωματιδίων) δημιουργήθηκε στα πλαίσια του προγράμματος LIFE09 ENV/GR/000289 και για το έργο "Ανάπτυξη ενός Εργαλείου άσκησης αποτελεσματικών πολιτικών για τη μείωση των αιωρούμενων σωματιδίων στον αέρα (ACEPT-AIR)"για τρεις αστικές περιοχές της Ελλάδας: την μητροπολιτική περιοχή της Αθήνας (ΜΠΑ), την μητροπολιτική περιοχή της Θεσσαλονίκης (ΜΠΘ) και την ευρύτερη περιοχή του Βόλου (ΕΠΒ). Η βάση δεδομένων αυτή περιλαμβάνει τα δεδομένα των κύριων χημικών συστατικών αλλά και των ιχνοστοιχείων που σχετίζονται με τα κλάσματα PM_{10} και $PM_{2.5,}$ τα οποία μετρήθηκαν κατά την διάρκεια του προγράμματος ACEPT-AIR, καθώς και σχετικά ιστορικά δεδομένα. Συγκεκριμένα η βάση δεδομένων περιέχει πληροφορίες για χημικά συστατικά των ΑΣ όπως: χημικά στοιχεία (κύρια και ιχνοστοιχεία συμπεριλαμβανομένων των βαρέων μετάλλων), ιοντικά συστατικά (SO_4^{-2}, NO_3^-, NH_4^+, Cl^-, Na^+, K^+, Ca^{2+}, Mg^{2+}), ανθρακούχα ύλη (OC και EC), οργανικές ενώσεις (PAHs, PCBs, OCPs, n-αλκάνια, κτλ).

Σχετικά με την ανθρακούχα ύλη, οι συγκεντρώσεις του οργανικού (OC) και στοιχειακού (EC) άνθρακα και στις δύο θέσεις στην Αθήνα, στο Βόλο και στην θέση αστικού υποβάθρου στην Θεσσαλονίκη, ήταν σχετικά χαμηλές κατά την θερμή περίοδο. Χαμηλός λόγος EC/OC στις θέσεις αστικού υποβάθρου υποδηλώνει χαμηλή επίδραση εκπομπών κίνησης οχημάτων, σε συνδυασμό με σχηματισμό δευτερογενών οργανικών ενώσεων. Στη θέση κυκλοφορίας της Θεσσαλονίκης, οι συγκεντρώσεις ήταν σημαντικά υψηλές, ανάμεσα στις υψηλότερες που έχουν αναφερθεί σε αστικές περιοχές της Ευρώπης. Κατά την ψυχρή περίοδο υπήρξε παρόμοια διακύμανση, με τις συγκεντρώσεις του OC να συνεισφέρουν το μεγαλύτερο ποσοστό στον ολικό άνθρακα σε όλες τις περιοχές. Η επίδραση των εκπομπών της οικιακής θέρμανσης ήταν εμφανείς την περίοδο αυτή λόγω των υψηλότερων συγκεντρώσεων OC και EC.

Οι χαμηλοί λόγοι συγκέντρωσης EC/OCκατά την ψυχρή περίοδο είναι ενδεικτικοί ΑΣ που προέρχονται από καύση βιομάζας, και υποδεικνύουν έντονη χρήση τζακιών.

Στις θέσεις της ΜΠΑ τα SO_4^{-2}, NO_3^-, NH_4^+και Ca^{2+}ήταν τα επικρατή ιοντικά είδη στα $ΑΣ_{10}$, ενώ στα $ΑΣ_{2.5}$ ήταν τα SO_4^{-2}, NO_3^-, NH_4^+. Τα ιόντα Cl^-, Na^+ και Ca^{2+} παρουσίασαν τους χαμηλότερους λόγους $ΑΣ_{2.5}/ΑΣ_{10}$. Λόγοι $ΑΣ_{2.5}/ΑΣ_{10}$ κοντά στο 1 παρατηρήθηκαν για τα SO_4^{2-} και NH_4^+ και στις δύο θέσεις στην ΜΠΑ. Ομοίως, στις θέσεις της ΜΠΘ τα SO_4^{-2}, NO_3^-, NH_4^+ και Ca^{2+} ήταν τα κύρια ιόντα στα $ΑΣ_{10}$ και τα SO_4^{-2}, NO_3^-, NH_4^+ στα $ΑΣ_{2.5}$. Τα NO_3^- , Cl^- και Ca^{2+} στα $ΑΣ_{2.5}$ είχαν ελαφρώς υψηλότερη συγκέντρωση στην θέση κυκλοφορίας, ενώ τα SO_4^{2-} ελαφρώς υψηλότερη συγκέντρωση στη θέση αστικού υποβάθρου. Οι υψηλότεροι λόγοι $ΑΣ_{2.5}/ΑΣ_{10}$ παρουσιάστηκαν για τα NH_4^+ (1.46-1.90), ενώ το Ca^{2+} παρουσίασε τους χαμηλότερους λόγους (0.16-0.22). Σε σχέση με όλες τις θέσεις δειγματοληψίας στον Βόλο παρουσιάστηκαν οι υψηλότερες συγκεντρώσεις για τα SO_4^{-2}, NH_4^+, K^+, Cl^-, Ca^{2+} στα $ΑΣ_{10}$, και για τα Na^+, K^+, Ca^{2+} και SO_4^{-2} στα $ΑΣ_{2.5}$.

Σε όλες τις θέσεις τα στοιχεία που προέρχονται από τον φλοιό της γης όπως τα Ca, Si, Fe, Al ήταν αυτά με την μεγαλύτερη συγκέντρωση ακολουθούμενα από αυτά που σχετίζονται με ανθρωπογενείς διεργασίες (K, S και Zn). Τα S, K και Ca ήταν τα στοιχεία με υψηλότερη συγκέντρωση στα $ΑΣ_{2.5}$. Το Ca βρέθηκε σε πολύ υψηλές συγκεντρώσεις στη θέση κυκλοφορίας στην ΜΠΘ και στο Βόλο, περιοχές και θέσεις στις οποίες ο λόγος Ca/Si ήταν ο υψηλότερος σε σχέση με τις υπόλοιπες (4.1 και 3, αντίστοιχα), υποδηλώνοντας την επίδραση διεργασιών δόμησης και οδοποιίας. Στον Βόλο παρατηρήθηκαν οι υψηλότερες συγκεντρώσεις στοιχείων με ανθρωπογενή προέλευση όπως τα Zn, S, K, As, Br, και Pb στα $ΑΣ_{10}$ και στα K, Ca, Fe, Cu, Zn, Pb, Mg, Al, Si, S, Cl, Mn και As στα $ΑΣ_{2.5}$.

Για να επιτευχθεί η διαδικασία της "χημικής αναδόμησης", τα χημικά συστατικά χωρίστηκαν σε έξι κατηγορίες: τα συστατικά του φλοιού της γης, τα ιχνοστοιχεία, την οργανική ύλη, το στοιχειακό άνθρακα, το θαλασσινό αλάτι και τα δευτερογενή ανόργανα σωματίδια. Τα δευτερογενή ανόργανα σωματίδια, η οργανική ύλη, και τα στοιχεία του φλοιού ήταν με διαφορά τα επικρατούντα συστατικά στα $ΑΣ_{10}$ σε όλες τις περιοχές ενώ αντίστοιχα στα $ΑΣ_{2.5}$ ήταν τα δευτερογενή ανόργανα σωματίδια και η οργανική ύλη. Σημαντική συνεισφορά από ανόργανο άνθρακα καταγράφηκε στη θέση κυκλοφορίας στη ΜΠΘ αγγίζοντας το 22% της μάζας των $ΑΣ_{2.5}$ την θερινή περίοδο. Η μη επιμερισμένη μάζα κυμάνθηκε μεταξύ 4%-17% στη ΜΠΑ, 13%-32% στη ΜΠΘ και 1%-37% στην ΕΠΒ.

Table of Contents

EXECUTIVE SUMMARY 2

ΠΕΡΙΛΗΨΗ 3

1. INTRODUCTION 6

2. METHODOLOGY 6

2.1. Description of the ACEPT-AIR project sampling sites 6

2.2 Sampling methods 8

2.3 Chemical speciation of PM_{10} and $PM_{2.5}$ 8

2.4. Description of the PM10 and PM2.5 ACEPT-AIR Database 9

3. RESULTS AND DISCUSSION 11

3.1. Carbonaceous species 11

3.2. Ionic components 12

3.3. Elemental species 14

3.4. Mass closure of PM_{10} and $PM_{2.5}$ particle fractions 16

References 21

ANNEX I: Concentration of major ionic components 23

ANNEX II: Concentration of major and trace elements 24

1. INTRODUCTION

A mass concentration and chemical composition Database was constructed in the framework of the LIFE09 ENV/GR/000289 project "Development of A Cost Efficient Policy Tool for reduction of Particulate Matter in AIR(ACEPT-AIR)" for particle fractions PM_{10} and $PM_{2.5}$ at three urban areas of Greece: the Athens Metropolitan Area (AMA), the Thessaloniki Metropolitan Area (TMA) and the Volos Greater Area (VGA).These data were then used for the source apportionment of ambient PM_{10} and $PM_{2.5}$ using receptor models. The Database also incorporated relevant historical data for the three study areas since 1990.

This report presents a description of the PM_{10} and $PM_{2.5}$ Chemical Composition Database and summarizes the concentrations of major and trace chemical constituents (ionic components, organic and elemental carbon, major and trace elements, etc.) that were determined in PM_{10} and $PM_{2.5}$ particle fractions in the framework of the ACEPT-AIR project.

2. METHODOLOGY

2.1. Description of the ACEPT-AIR project sampling sites

The ACEPT-AIR project was concurrently carried out at 2 sites in the Athens Metropolitan Area (Figure 1), at two sites in the Thessaloniki Metropolitan Area (Figure 2), and at one site in the Volos Greater Area (Figure 3). A detailed description of sampling sites is provided in the Report of D6 "PM_{10} and $PM_{2.5}$ Concentration Databases for the three urban areas AMA, TMA and VGA".

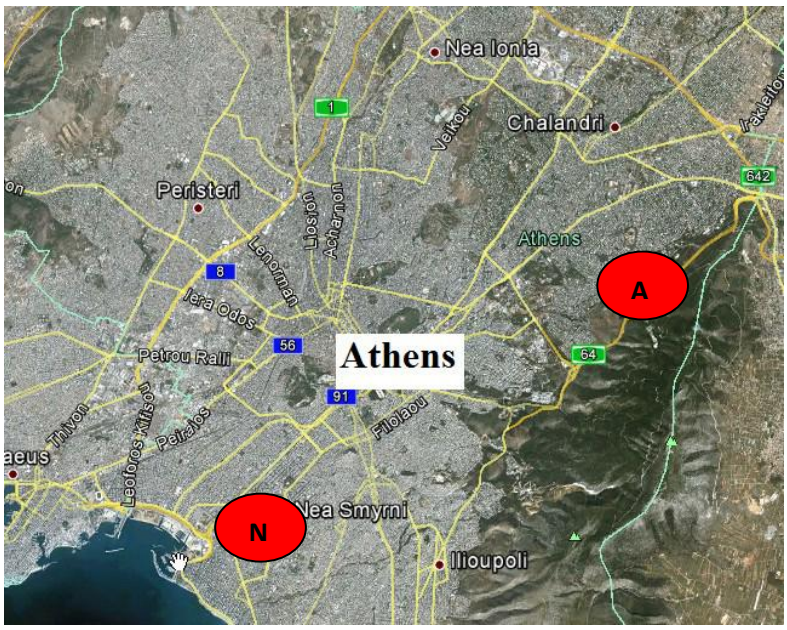

Figure 1 Map of the AMA (Athens Metropolitan Area) with the ACEPT-AIR sampling sites (AP: AgiaParaskevi, NS: NeaSmyrni).

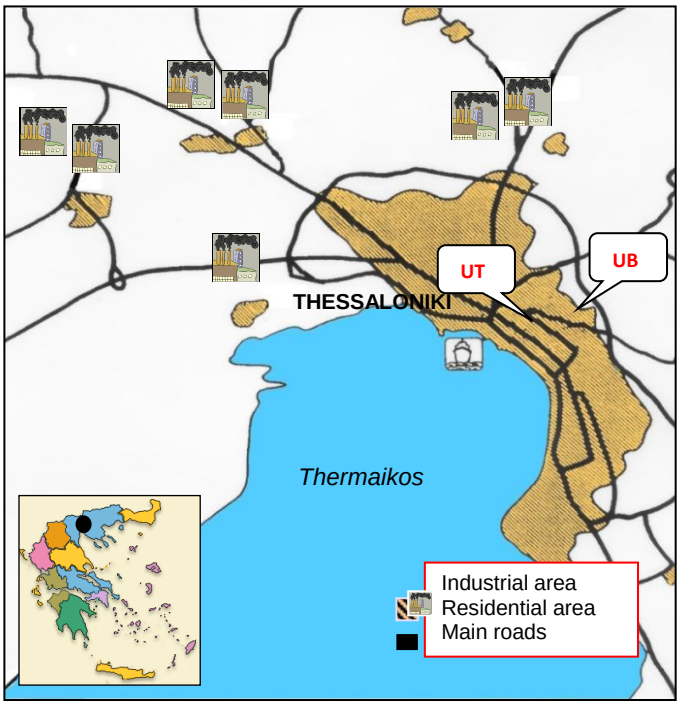

Figure 2 Map of the Thessaloniki Metropolitan Area with the ACEPT-AIR sampling sites (UT: urban-traffic, UB: urban background).

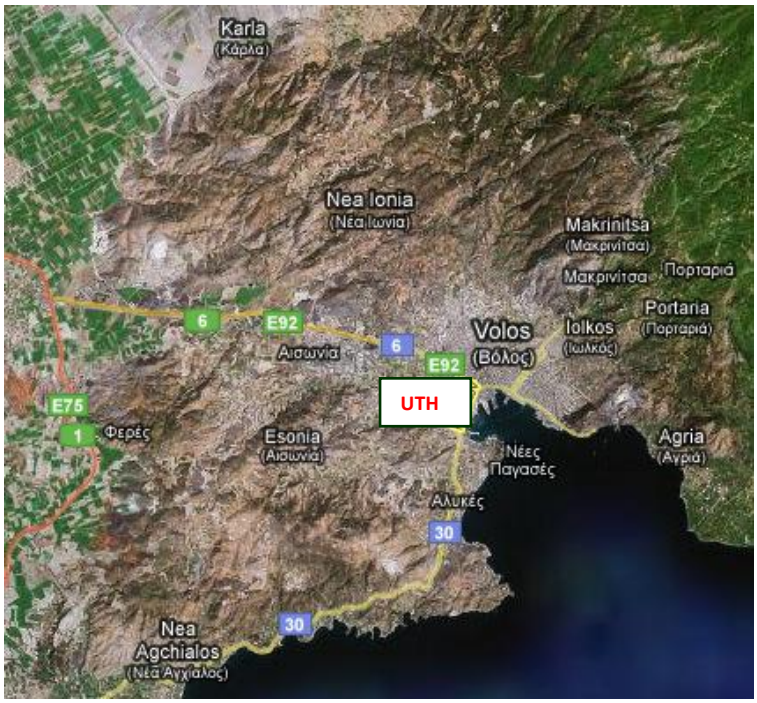

Figure 3 Map of the Volos Greater Area with the ACEPT-AIR sampling site at the University of Thessaly (UTH).

2.2 Sampling methods

At all sites, PM_{10} and $PM_{2.5}$ sampling was carried out concurrently according to the reference methods ISO/IEC EN-12341 and ISO/IEC EN-14907, respectively, using low volume air samplers equipped with PM_{10} and $PM_{2.5}$ inlets that were operated at constant flow rate of 2.3 m^3/h. Each PM_{10}/$PM_{2.5}$ sampling had a 24-h duration. Each PM fraction was concurrently collected on two filter media: Φ 47 mm Teflon filter (Zefluor^{TM}membranes, Pall 2μm) for subsequent analysis of elements and ionic species, and Φ 47 Quartz filter (Tissuquartz, Pall) for subsequent analysis of organic and elemental carbon, OC and EC. Details about sampling methods are provided in Deliverable D6 "PM_{10} and $PM_{2.5}$ Concentration Databases for the three urban areas AMA, TMA and VGA".

2.3 Chemical speciation of PM_{10} and $PM_{2.5}$

A summary description of the methods used for chemical speciation of PM_{10} and $PM_{2.5}$ samples is provided in Table 1.

Table 1 Summary description of the methods used for chemical analysis of PM_{10} and $PM_{2.5}$ samples.

Chemical class	Chemical components	Sample preparation	Analytical method
Carbonaceous species	OC, EC	-	TOT
Ionic species	SO_4^{2-},NO_3^-,NH_4^+ Na^+, K^+, Cl^-, Ca^{2+},Mg^{2+}	Aqueous extraction	IC
Major and trace elements	Mg, Al, Si, S, Cl, K, Ca, Ti, V, Mn, Fe, Ni, Cu, Zn, As, Br, Sr, Ba, Pb	-	ED-XRF
Trace elements	V, As, Sb, Co, Cr, Cd	Digestion with HNO_3^- / HCl mixture	GF-AAS

TOT: Thermal Optical Transmission Analysis; IC: Ion Chromatography; ED-XRF: Energy Dispersive X-Ray Fluorescence; GF-AAS: Graphite Furnace Atomic Absorption Spectroscopy

2.4. Description of the PM10 and PM2.5 ACEPT-AIR Database

All the data collected in the framework of the project (both historical and current) have been introduced into a Database which is submitted as a Deliverable for Action 2. The ACEPT-AIR Database provides information for PM_{10} and $PM_{2.5}$ mass and particle chemical composition for the Athens Metropolitan Area (AMA), the Thessaloniki Metropolitan Area (TMA), and the Volos Greater Area (VGA). Briefly, the Database has two similar structured platforms:

- The **Historical Data** platform, that includes concentrations for PM mass and chemical constituents measured at various sites within the aforementioned areas during the period 2000-2010. Sources of these data were previous measurements by ACEPT-AIR partners, records of the air pollution monitoring stations operated by national and local authorities (Greek Ministry of Environment, Municipality of Thessaloniki, etc), as well as published data of independent researchers. The historical data were collected in the framework of the project and were examined with respect to sampling protocols, sampling and analytical methods and data analysis. After being submitted tostrict quality control procedures, the collected data have been introduced in the historical database.
- The **LIFE Data** platform**,** that includes concentrations of PM_{10} and $PM_{2.5}$ and their associated chemical components measured during 2011-2012 in the framework of the ACEPT-AIR project.

The user can have access to the data by selecting various options regarding the identity and characteristics of the sampling site, such as the study area (the user can select among the Athens Metropolitan Area (AMA), the Thessaloniki Metropolitan Area (TMA), and the Volos Greater Area (VGA)), the specific station in each area (by this selection, a map from Google maps also comes into view), the authority responsible for the station, the characterization of the station regarding its distance from various sources (i.e. urban-traffic, urban background, industrial), and the gaseous pollutants measured at the station (CO, NOx, SO_2, O_3, etc).
In addition to PM mass, the Database provides information for major and trace chemical components of PM, such as:

- elemental components (major and trace elements including heavy metals)
- ionic components (SO_4^{-2}, NO_3^-, NH_4^+, Cl^-, Na^+, K^+, Ca^{2+}, Mg^{2+})
- carbonaceous species (OC and EC)
- organic compounds (PAHs, PCBs, OCPs, n-alkanes, etc).

The user can choose information for all data within a chemical class or for specific chemical parameters (e.g. for individual elements, ionic species, etc) (Figures 4 and 5). Then, a table appears with the selected data for each year.

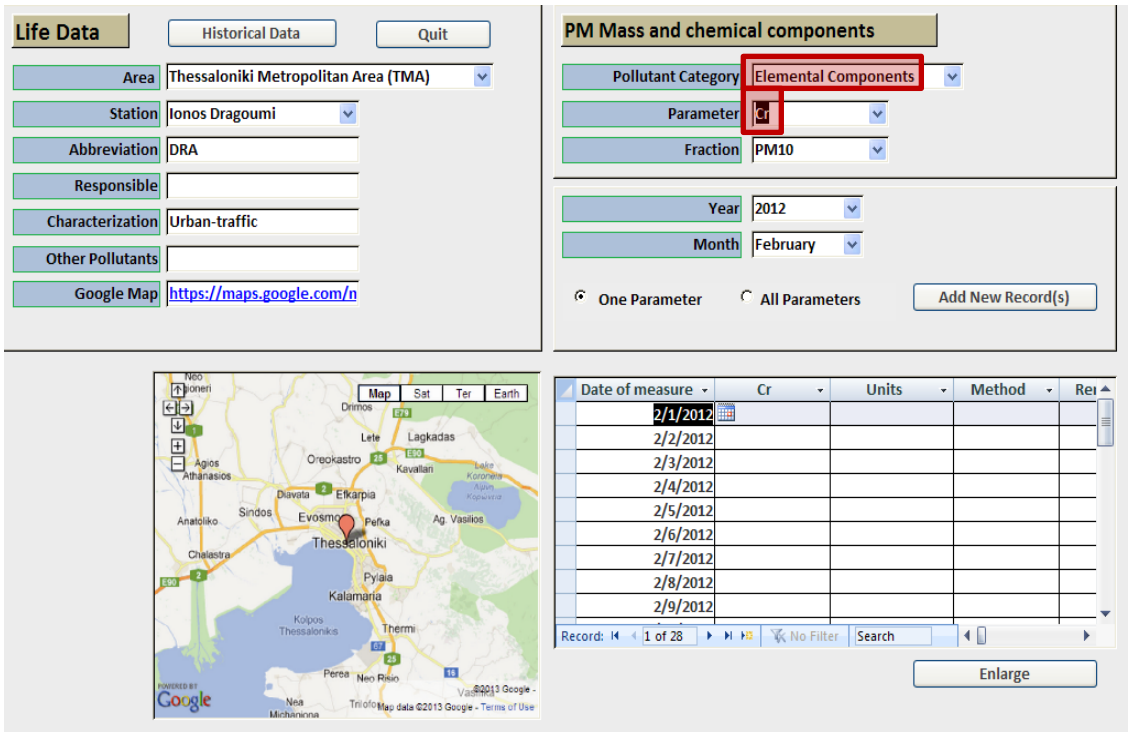

Figure 4 LIFE data for Cr bound to PM_{10} at the Ionos Dragoumi station (urban traffic site in TMA, TMA-UT site).

Date of mea	PM	Mg	Al	Si	S	Ti	V	Cr	Mn	Fe	Co	Ni	Cu	Zn
7/1/2011	#	#	#	#	#	#	#	#	#	#	#	#	#	
7/2/2011	29	141.2	252.8	590.1	887.6	25.8	nd	16.5	22.7	914.8	8.01	3.2	27.7	
7/3/2011	#	#	#	#	#	#	#	#	#	#	#	#	#	
7/4/2011	29.1	132.2	262.1	633.4	680.3	27.7	4.76	12.0	28.2	951.6	1.50	7.2	31.6	
7/5/2011	#	#	#	#	#	#	#	#	#	#	#	#	#	
7/6/2011	50.7	244.2	405.9	854.0	1064.4	47.6	5.30	15.9	26.0	1367.0	6.67	3.6	55.0	
7/7/2011	#	#	#	#	#	#	#	#	#	#	#	#	#	
7/8/2011	42.1	86.9	131.0	286.1	2693.3	11.3	8.35	2.1	22.4	364.3	4.54	5.5	24.3	
7/9/2011	#	#	#	#	#	#	#	#	#	#	#	#	#	
7/10/2011	54.8	283.2	610.6	1258.9	1916.6	39.7	nd	17.3	115.5	962.2	3.21	3.1	26.5	
7/11/2011	#	#	#	#	#	#	#	#	#	#	#	#	#	
7/12/2011	61.3	541.6	986.2	2135.5	1389.7	66.8	nd	18.0	115.5	1837.0	6.29	11.7	59.4	
7/13/2011	#	#	#	#	#	#	#	#	#	#	#	#	#	
7/14/2011	44.0	255.9	564.7	1268.0	1592.9	52.4	6.33	11.1	55.8	1273.6	6.76	4.2	40.6	
7/15/2011	#	#	#	#	#	#	#	#	#	#	#	#	#	
7/16/2011	51.7	477.3	806.0	1723.7	1840.0	64.3	nd	16.8	89.6	1470.9	10.10	16.6	28.2	
7/17/2011	#	#	#	#	#	#	#	#	#	#	#	#	#	
7/18/2011	50.3	329.4	997.6	2072.7	1495.1	55.7	nd	8.3	76.0	1331.5	10.31	5.0	32.9	
7/19/2011	#	#	#	#	#	#	#	#	#	#	#	#	#	
7/20/2011	52.7	388.1	952.0	2130.2	1394.4	67.8	5.28	17.8	60.7	1551.5	6.51	7.9	44.0	
7/21/2011	#	#	#	#	#	#	#	#	#	#	#	#	#	
7/22/2011	#	#	#	#	#	#	#	#	#	#	#	#	#	
7/23/2011	#	#	#	#	#	#	#	#	#	#	#	#	#	
7/24/2011	29.2	302.9	585.3	1169.9	947.0	46.7	7.40	12.5	56.9	944.9	10.42	4.5	25.7	
7/25/2011	#	#	#	#	#	#	#	#	#	#	#	#	#	
7/26/2011	#	#	#	#	#	#	#	#	#	#	#	#	#	
7/27/2011	#	#	#	#	#	#	#	#	#	#	#	#	#	
7/28/2011	#	#	#	#	#	#	#	#	#	#	#	#	#	
7/29/2011	51.4	147.2	154.1	363.1	3405.2	12.3	25.26	2.7	37.8	419.2	5.16	8.8	22.5	
7/30/2011	#	#	#	#	#	#	#	#	#	#	#	#	#	
7/31/2011	33.9	236.8	426.1	865.2	1572.6	36.2	4.93	11.8	31.5	872.6	2.75	1.9	30.1	

Figure 5 LIFE data for elemental components associated to PM_{10} at the urban background site in TMA (TMA-UB).

3. RESULTS AND DISCUSSION

3.1. Carbonaceous species

Summary statistical data for 24-hr concentrations of carbonaceous species, organic carbon (OC) and elemental carbon (EC) associated with PM_{10} and $PM_{2.5}$ are given in Tables 2 and 3 for the warm and the cold period, respectively.

OC and EC concentrations at both Athens sites and at Volos and Thessaloniki background site were relatively low during the warm period. The background character of the stations was further demonstrated by the low EC/OC ratios indicating relatively low contribution from traffic emissions, coupled with secondary organic formation which enhances OC levels. At the traffic site in Thessaloniki, concentrations were significantly higher, among the highest values reported for other urban sites in European cities (Grivas et al. 2012; Viana et al. 2006). The corresponding EC/OC ratio was around 1.0, similar to those found at kerbside sites and close to the ratio values reported for vehicular emissions (Samara et al., 2013).

Table 2 Summary statistical data for 24-hr PM_{10} and $PM_{2.5}$ bound organic (OC) and elemental (EC) carbon concentration during the warm period [μg m^{-3}].

PM_{10}						
	OC		**EC**		**OC/EC**	
Area/Site	***Mean±SD***	***Range***	***Mean±SD***	***Range***	***Mean±SD***	***N***
AMA/AP	2.7±1.0	1.1-5.9	0.3±0.2	0.1-0.8	10.8±4.8	21
AMA/NS	4.4±1.5	1.7-8.1	0.8±0.4	0.2-1.9	6.3±2.6	44
TMA/UT	8.6±2.7	4.4-16.4	7.8±1.4	5.5-10.4	1.1±0.4	27
TMA/UB	4.1±1.7	1.7-7.2	0.7±0.3	0.1-1.4	6.2±2.2	26
VGA/UTH	4.6±1.1	2.6-6.9	0.8±0.4	0.3-1.6	6.8±2.6	9
$PM_{2.5}$						
	OC		**EC**		**OC/EC**	
Area/Site	***Mean±SD***	***Range***	***Mean±SD***	***Range***	***Mean±SD***	***N***
AMA/AP	2.7±1.0	1.0-5.9	0.3±0.2	0.1-0.8	10.0±4.9	48
AMA/NS	3.2±1.0	0.6-6.3	0.6±0.3	0.1-1.7	6.0±2.7	49
TMA/UT	6.0±2.3	3.0-12.6	5.9±1.3	3.7-9.2	1.1±0.5	28
TMA/UB	3.3±1.3	1.2-5.4	0.5±0.2	0.1-0.8	7.1±2.6	27
VGA/UTH	3.7±1.0	2.0-6.0	0.6±0.2	0.2-1.2	6.6±1.9	28

Cold period data presented a similar pattern with OC concentrations contributing the most to total carbon at all sites. Even the traffic site in Thessaloniki presented OC/EC ratios higher than 1.0 (around 3.0). The effect of residential heating during this period was apparent in the much higher OC and EC concentrations. Very high mean 24-hr concentrations (OC reaching up to 45 μg m^{-3} and EC up to 6 μg m^{-3}) were measured in the densely populated area of Nea Smyrni. The high values of OC/EC concentration ratios during cold season are indicative of biomass burning aerosol and suggest intense use of fireplaces during this season.

Table 3 Summary statistical data for 24-hr PM_{10} and $PM_{2.5}$ bound organic (OC) and elemental (EC) carbon concentration during the cold period [μg m^{-3}].

PM_{10}						
	OC		**EC**		**OC/EC**	
Area/Site	***Mean±SD***	***Range***	***Mean±SD***	***Range***	***Mean±SD***	***N***
AMA/AP	4.1±1.5	1.0-8.5	0.5±0.2	0.1-1.3	8.7±2.9	47
AMA/NS	9.3±7.9	1.7-44.6	1.4±1.0	0.4-6.0	7.1±2.4	50
TMA/UT	14.2±5.3	4.9-23.0	5.5±2.3	2.5-11.2	2.8±1.0	30
TMA/UB	8.7±5.0	3.4-21.0	1.2±0.8	0.3-3.3	8.3±2.4	27
VGA/UTH	10.8±4.5	4.4-18.0	1.5 ± 1.0	0.4-3.8	8.7±3.5	25
$PM_{2.5}$						
	OC		**EC**		**OC/EC**	
Area/Site	***Mean±SD***	***Range***	***Mean±SD***	***Range***	***Mean±SD***	***N***
AMA/AP	4.0±1.5	1.0-7.9	0.4±0.2	0.1-1.0	10.1±3.3	49
AMA/NS	8.9±7.6	1.7-41.8	1.2±0.9	0.3-4.0	7.5±2.5	45
TMA/UT	11.1±4.0	4.8-23.0	4.5±1.4	2.5-8.3	2.8±1.5	30
TMA/UB	8.7±5.0	2.8-21.0	0.9±0.4	0.3-1.9	9.4±2.3	27
VGA/UTH	10.0±4.0	3.8-18.0	1.2±0.7	0.3-3.5	9.7±2.7	25

3.2. Ionic components

Mean ionic component concentrations in PM_{10} and $PM_{2.5}$ during the warm and the cold season are presented in Figures 6-8.

At the AMA sites (Figure 6), SO_4^{-2}, NO_3^-, NH_4^+ and Ca^{2+} were the prevalent ions in the PM_{10} fraction *vs.* SO_4^{-2}, NO_3^-, NH_4^+ in the $PM_{2.5}$ fraction. In general, concentrations were slightly higher at NS, except for Na^+ and Cl^- (sea salt) which were more abundant in PM_{10} measured at AP site. Cl^-, Na^+ and Ca^{2+}exhibited the lowest $PM_{2.5}/PM_{10}$ ratios. $PM_{2.5}/PM_{10}$ ratio values close to 1 were found for $SO_4^{2-}$and NH_4^+at both sites, while NO_3^- presented a significant coarse fraction as well (mean

$PM_{2.5}/PM_{10}$ ratio equal to 0.20 and 0.54 in AP and NS respectively). This result, along with a good correlation between NO_3^- and Cl^- with Na^+ suggest (especially for AP), suggests neutralization of NO_3^- with Na^+ from sea salt, which is mainly found in coarse mode (Eleftheriadis et al., 2014).

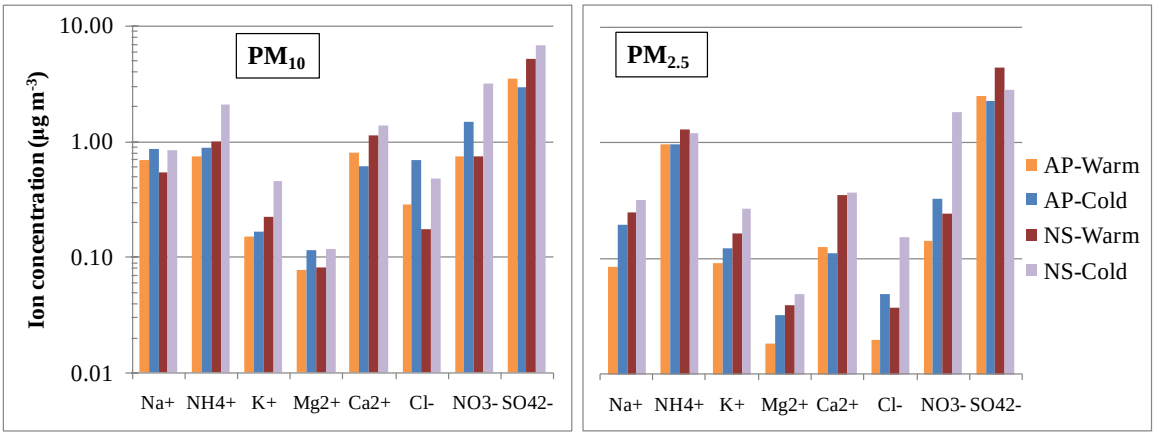

Figure 6 Mean ionic component concentrations (logarithmic scale) in PM_{10} and $PM_{2.5}$ during the warm and the cold season at the two sites in AMA.

Similarly, at the TMA sites (Figure 7), SO_4^{-2}, NO_3^-, NH_4^+ and Ca^{2+} were the major ions in the PM_{10} fraction *vs.* SO_4^{-2}, NO_3^-, NH_4^+ in the $PM_{2.5}$ fraction. NO_3^-, Cl^- and Ca^{2+} associated to $PM_{2.5}$ were slightly higher at the UT site, whereas SO_4^{2-} slightly higher at the UB site. Similar results have been reported from previous published works (Tsitouridiou et al., 2003; Samara & Tsitouridou, 2000). The highest $PM_{2.5}/PM_{10}$ ratios were found for NH_4^+ (1.46-1.90), while Ca^{2+}exhibited the lowest $PM_{2.5}/PM_{10}$ ratios (0.16-0.22). $PM_{2.5}/PM_{10}$ ratios with value greater than 1 are not uncommon for NH_4^+. Theodosi et al. (2011) have also observed lower values of NH_4^+ in PM_{10} compared to $PM_{2.5}$ and PM_1. Volatilization of NH_4Cl from the filter, formed by reaction of NH_4NO_3 and NaCl has been proposed to explain the NH_4^+ behavior (NH_4NO_3 +NaCl→NH_4Cl+$NaNO_3$). Since sea salt (and NaCl) is mainly associated with coarse particles, this negative artifact formation is mainly expected in PM_{10}. $PM_{2.5}/PM_{10}$ ratio values close to 1 were found for SO_4^{2-} at both sites and seasons and for NO_3^- at both sites in winter.

In Volos (Figure 8) again secondary ions (SO_4^{-2}, NH_4^+, and NO_3^-) contributed the most to PM_{10} and $PM_{2.5}$ mass, while Ca^{2+} concentration was also significant in PM_{10}. Concentration levels were similar to the ones measured in the large urban centers of Athens and Thessaloniki.

Regarding seasonal variability, the concentrations of $PM_{2.5}$-bound SO_4^- were elevated in summer at both sites in AMA suggesting increased photochemical formation of sulfates. K^+ was more abundant in $PM_{2.5}$ during cold season, which could be related to biomass combustion for residential heating as discussed above (section 3.1). NO_3^- concentrations were also much higher during cold season. This is expected in the countries around the Mediterranean where high temperatures and dry conditions

during the summer may lead to the decomposition of NH_4NO_3 in gaseous HNO_3 and NH_3.

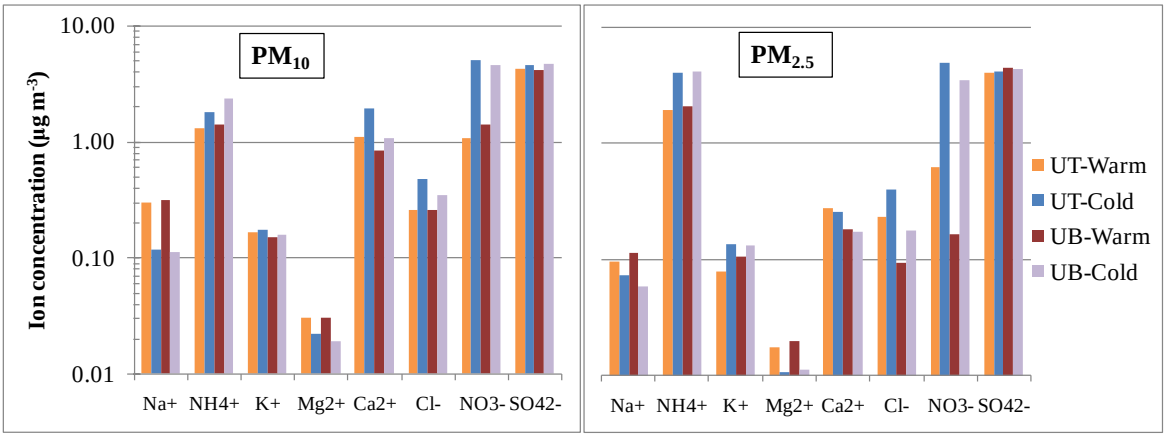

Figure 7 Mean ionic component concentrations (logarithmic scale) in PM_{10} and $PM_{2.5}$ during the warm and the cold season at the two sites in TMA.

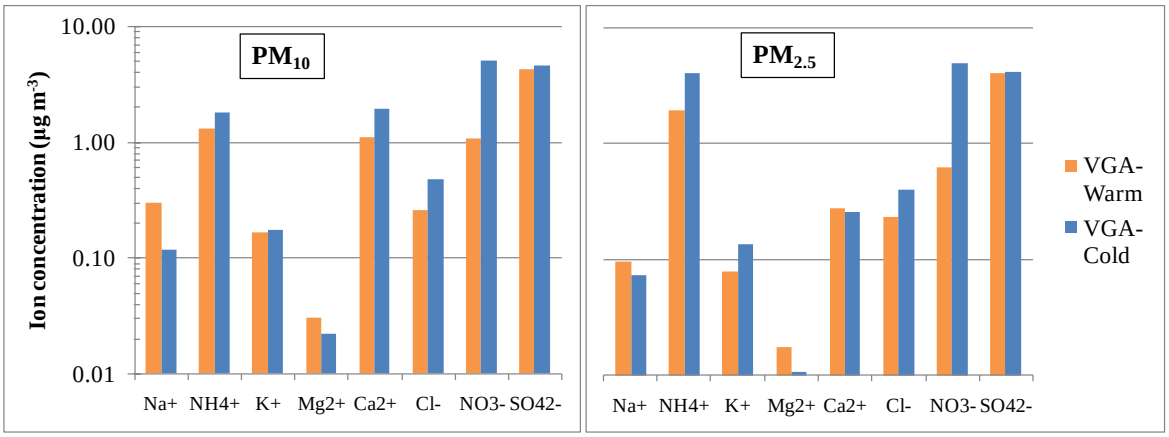

Figure 8 Mean concentration of major ions in PM_{10} and $PM_{2.5}$ in VGA during warm and cold season.

3.3. Elemental species

The annual mean concentrations of major and trace elements associated to PM_{10} and $PM_{2.5}$ particle fractions at the various sampling sites are shown in Figures 9 and 10, respectively.

At all sites, crustal elements, such as Ca, Si, Fe, Al were the most abundant elemental components in PM_{10} followed by elements related to anthropogenic processes (K, S and Zn). S, K and Ca were the prevalent elements in $PM_{2.5}$. The traffic site in TMA (UT) presented higher concentration levels of minerals and most trace metals in relation to the background site (UB) suggesting a stronger impact from traffic-related sources (road dust resuspension, brake and tire abrasion, road wear (Grigoratos et al.,

2014). In addition, Ca was found in predominantly high concentrations, particularly at TMA-UT and VGA, where the Ca/Si ratio was highest (4.1 and 3, respectively) indicating influence from construction sites and road works (at the time of the study the construction of the subway of Thessaloniki was in progress) and/or influence from industrial cement production (Voutsa et al., 2002). The high Ca/Si ratio favors nitrate and sulfate formation, since Ca rich soil dust is able to incorporate large amounts of precursor gases.

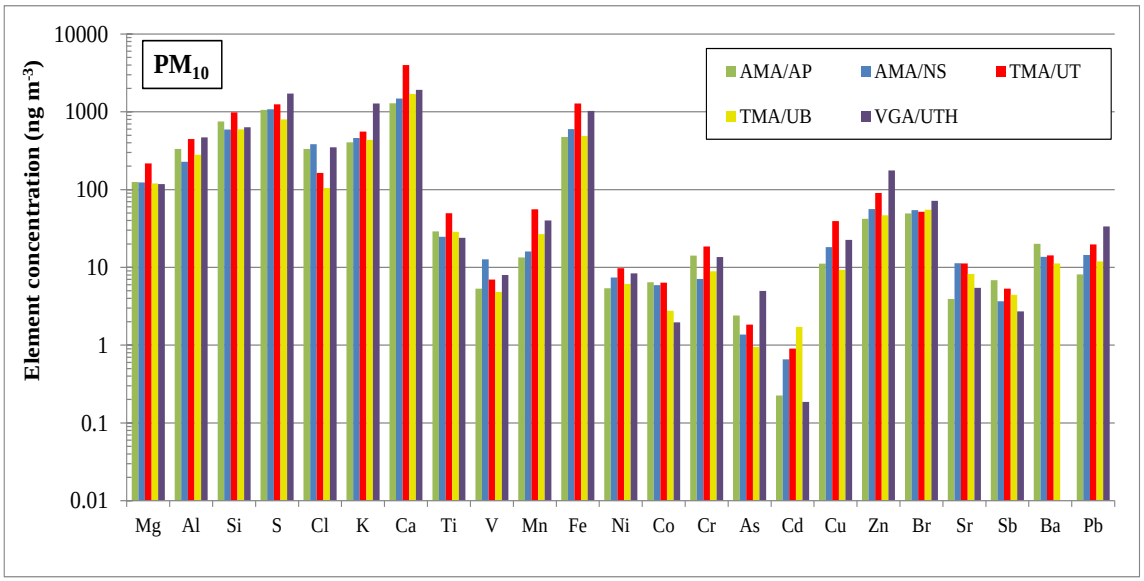

Figure 9 Elemental concentrations (logarithmic scale) in PM_{10} at the various sampling sites.

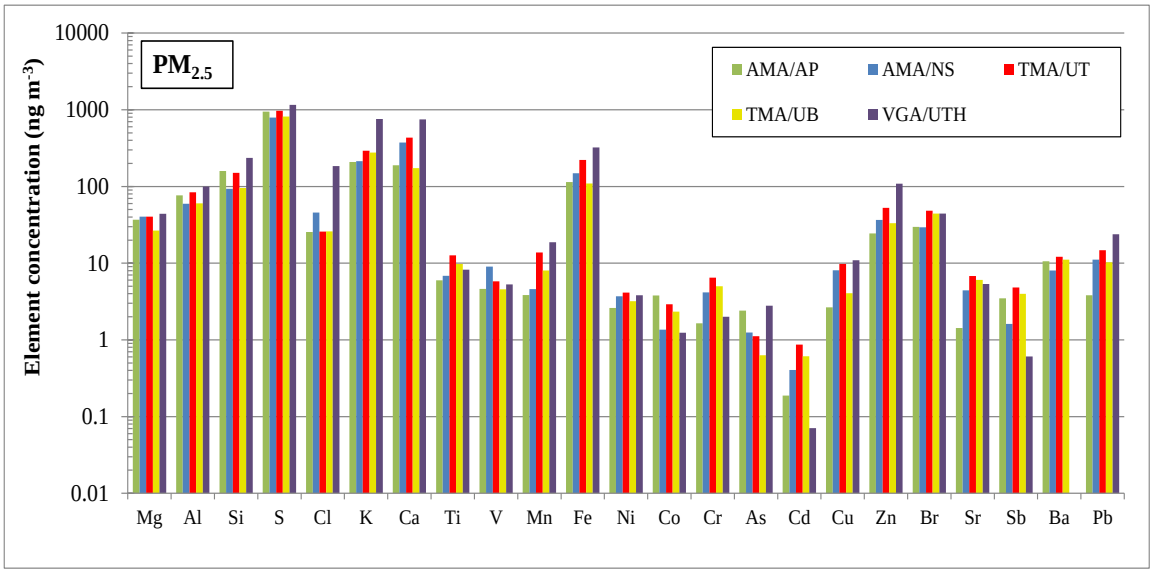

Figure 10 Elemental concentrations (logarithmic scale) in $PM_{2.5}$ at the various sampling sites.

Volos among all sampling sites presented the highest concentrations for anthropogenic elements such as Zn, S, K, As, Br, and Pb in PM_{10}, as well as the

highest concentrations for K, Ca, Fe, Cu, Zn, Pb, Mg, Al, Si, S, Cl, Mn and As in $PM_{2.5}$.

3.4. Mass closure of PM_{10} and $PM_{2.5}$ particle fractions

Mass closure, that is the reconstruction of PM mass through the determined particle chemical components, allows for a first insight into the sources affecting the concentration levels (Terzi et al., 2010). For this purposes, the chemical components were classified into the following categories based on expected origin: sea salt, minerals, trace elements, organic matter (OM), elemental carbon (EC), and secondary inorganic aerosol (SECONDARY). The difference between total PM mass and the sum of masses on the above classes provided the unidentified mass (UN), which corresponds to samples' water content and species not measured.

The sea salt (ss) contribution was calculated assuming that soluble Cl^- in aerosol samples comes solely from sea salt. Non sea salt sodium ($nssNa^+$) was calculated based on the crustal ratio Na^+/Al and total sea salt mass was calculated as the sum of Cl-, $ssNa^+$ and fractions of the concentrations of Mg^{2+}, K^+, Ca^{2+}, and SO_4^- based at a standard sea water concentration of these species with respect to sodium. The final equation used for the calculation of sea salt in PM mass was:

$$\text{Sea salt} = [Cl^-] + [Na^+] - [nssNa^+] + [ssMg^{2+}] + [ssK^+] + [ssSO_4^{2-}] =$$

$$= [Cl^-] + \{[Na^+] - 0.348 \times [Al]\} \times (1 + 0.119 + 0.037 + 0.038 + 0.253)$$

Minerals are the sum of Al, Si, Ca, Ti and Fe plus non sea salt Na^+, Mg and K, all multiplied by factors to convert them to their common oxides. Ca was multiplied by a factor of 1.95 to account for CaO and $CaCO_3$ which are considered as its most abundant forms. The final equation used for the calculation of the mineral part of PM was:

$$\text{Minerals} = [nssNa+] \times 1.35 + [nssMg] \times 1.66 + [Al] \times 1.89 + [Si] \times 2.14 + [nssK] \times 1.21 + [Ca] \times 1.95 + [Ti] \times 1.67 + [Fe] \times 1.43$$

Trace elements only represent a small percentage of the PM total mass; however they were also added to the analysis because they have a great environmental importance due to their toxicity and anthropogenic origin.

In order to include the oxygen, nitrogen and hydrogen associated with OC, OC was converted to organic matter (OM) using an average mean molecular to carbon ratio of 1.3-2 according the characteristics of each area and site. The ratio used varies according to the age of the organic matter. Fresh organic matter is often estimated using lower ratios while for the calculation of aged, more oxidized OM higher ratios are used. OM is expected to have higher emission rates on the traffic sites and lower

on urban background sites. In some extreme cases, such as aerosols impacted by heavy smoke, even higher conversion factors (2.2-2.6) can be used (Turpin & Lim, 2001). The equation used for OM calculation was:

$OM = [OC] \times f$, where $f = 1.3 - 2$

Finally, secondary inorganic aerosol was calculated as the sum of non-sea salt SO_4^{-2}, NO_3^-, and NH_4^+. The equation used was:

$$SECONDARY = [nssSO_4^{2-}] + [NO_3^-] + [NH_4^+] =$$

$$= [SO_4^{2-}] - 0.253 \times [ssNa^+] + [NO_3^-] + [NH_4^+]$$

The relative contributions of identified chemical classes to PM_{10} and $PM_{2.5}$ mass during the winter and summer campaigns are shown in Figures 11-15.

Secondary inorganic aerosol, OM, and minerals dominated the PM_{10} profiles at the two sites in AMA, at the UB site in TMA and in Volos. Similar results have been reported by other research works (Pateraki et al., 2014). At the UT site in TMA EC contribution was also significant. Sea salt contribution was larger in AMA (4-8%) with respect to TMA and VGA (1-2%) (Voutsa et al., 2014). In $PM_{2.5,}$ secondary aerosol and OM were the prevalent components. Mineral contribution was larger during warm season when dry conditions favor soil dust resuspension, while OM was significantly higher during cold season, pointing towards biomass burning for residential heating. EC also increased during cold season, especially to the densely populated areas of NS and in VGA.

Unidentified mass (UN) ranged between 4%-17% in AMA, 13%-32% in TMA and 1%-37% in VGA. UN is usually attributed to the water content of PM and/or to approximations associated with the estimation of the organic matter amount and with the composition of crustal materials. Depending on particle composition, particle-bound water may constitute up to 20-30% of total PM mass (Canepari et al., 2013).

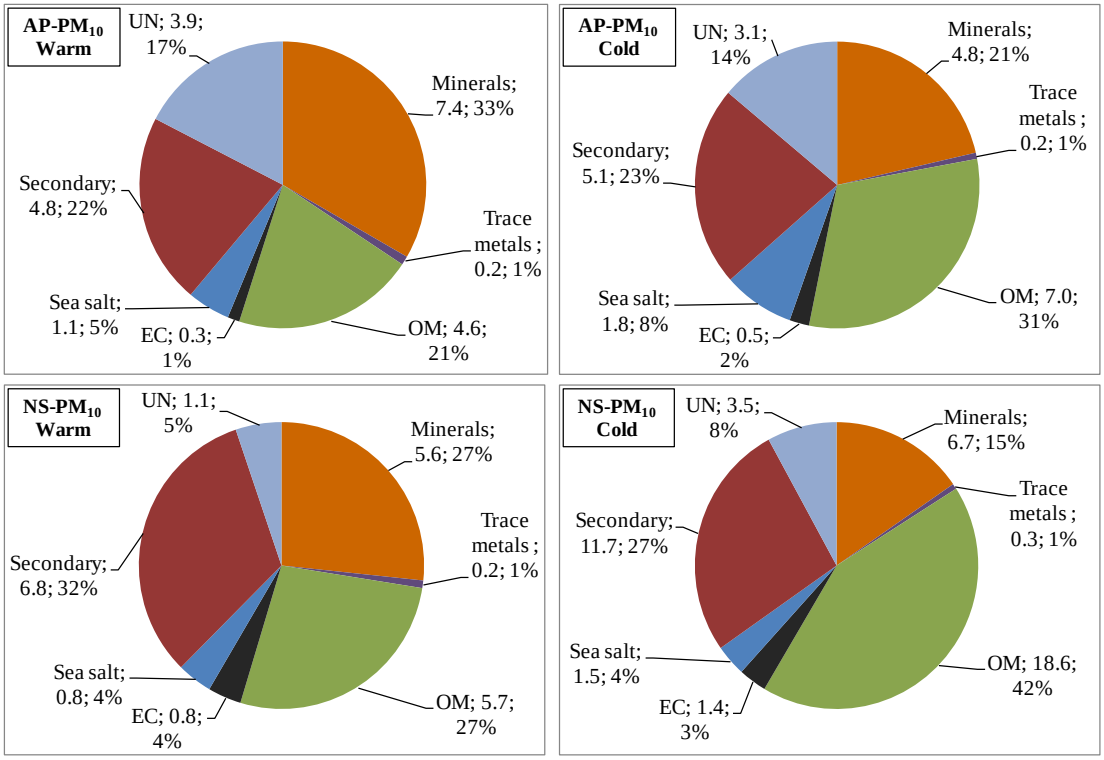

Figure 11 Mass closure of PM_{10} particle fraction in AMA; the first number corresponds to the mass [μg m^{-3}] of each chemical class and the second to its relative contribution [%] to total PM mass.

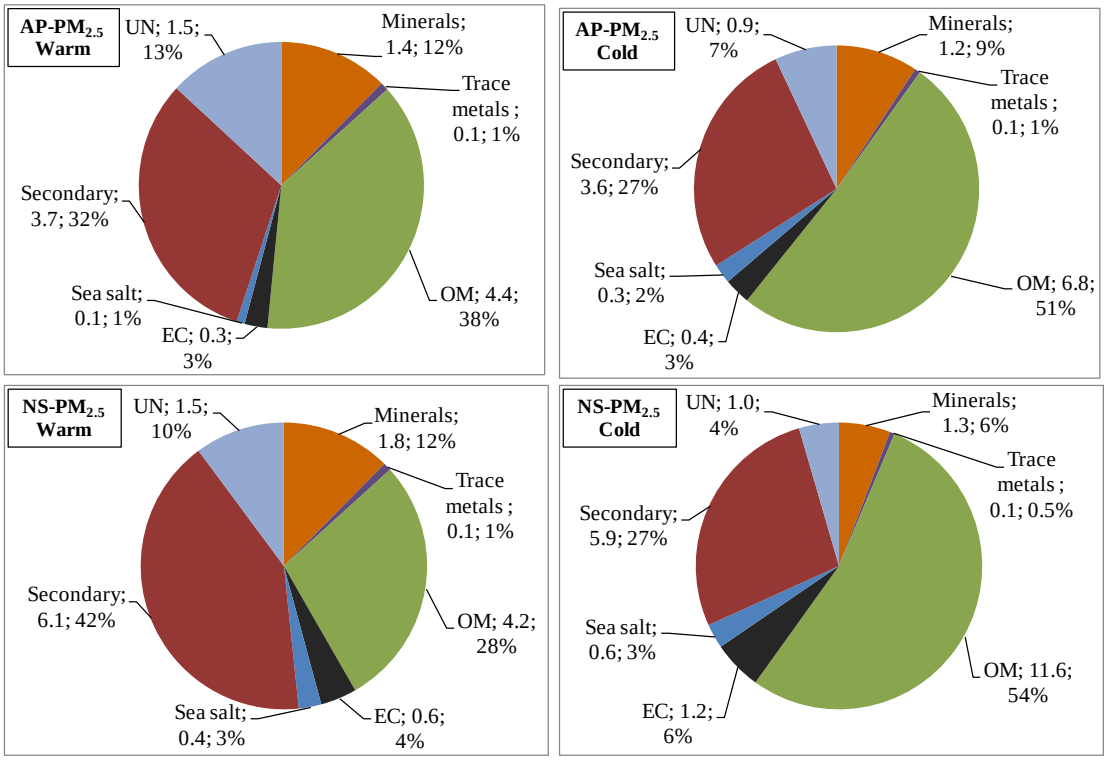

Figure 12 Mass closure of $PM_{2.5}$ particle fraction in AMA; the first number corresponds to the mass [μg m^{-3}] of each chemical class and the second to its relative contribution [%] to total PM mass.

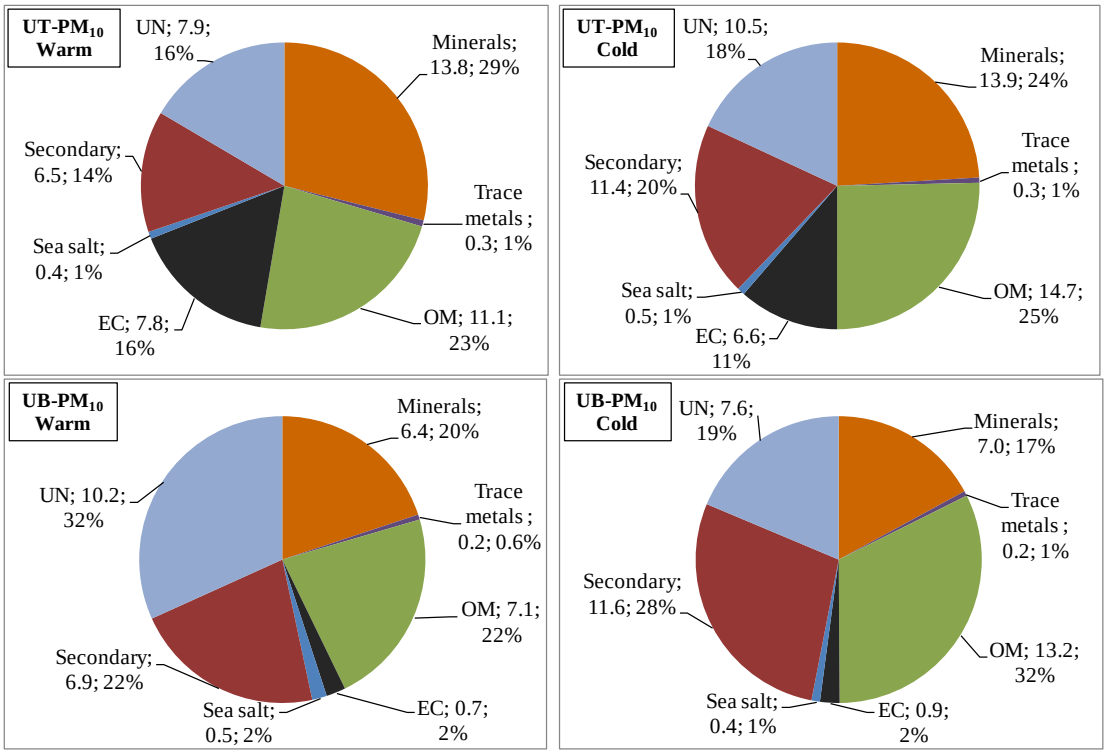

Figure 13 Mass closure of PM_{10} particle fraction in TMA; the first number corresponds to the mass [μg m^{-3}] of each chemical class and the second to its relative contribution [%] to total PM mass.

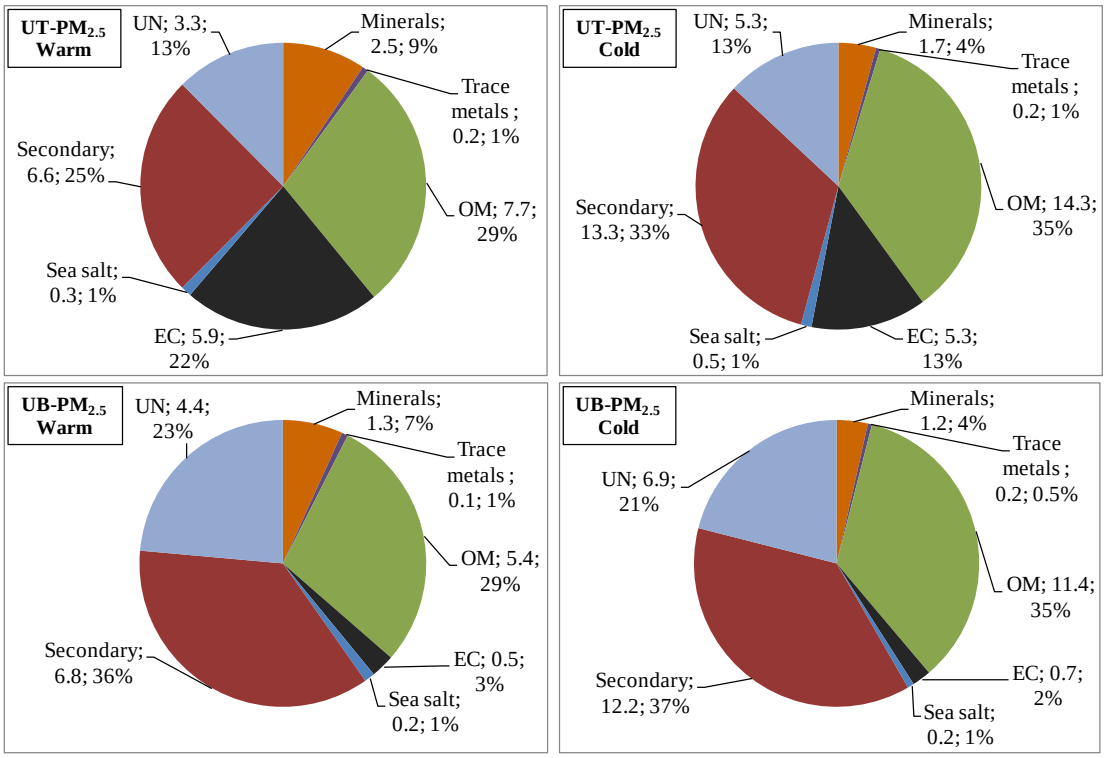

Figure 14 Mass closure of $PM_{2.5}$ particle fraction in TMA; the first number corresponds to the mass [μg m^{-3}] of each chemical class and the second to its relative contribution [%] to total PM mass.

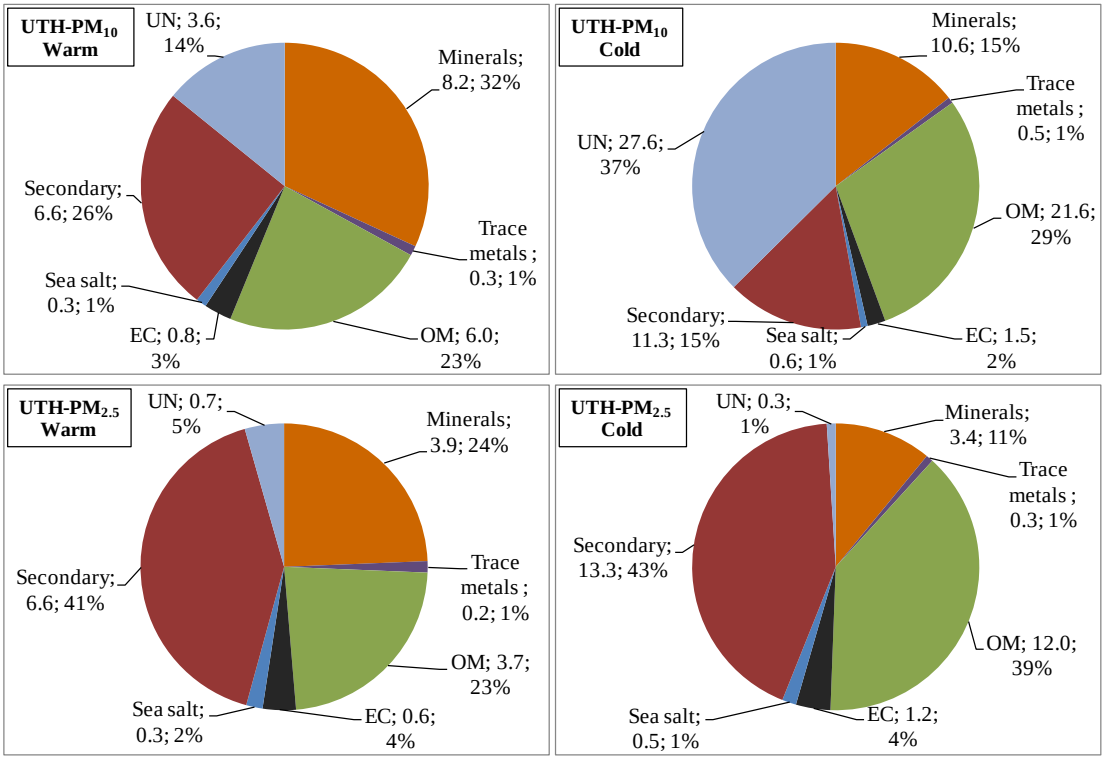

Figure 15 Mass closure of PM_{10} and $PM_{2.5}$ particle fractions in VGA; the first number corresponds to the mass [μg m^{-3}] of each chemical class and the second to its relative contribution [%] to total PM mass.

References

Canepari S., Farao C., Marconi E., Giovannelli C., Perrin C., (2013), Qualitative and quantitative determination of water in airborne particulate matter. Atmos. Chem. Phys., 13: 1193–1202.

Eleftheriadis K. , Ochsenkuhn K.M., Lymperopoulou Th., Karanasiou A., Razos P., Ochsenkuhn-Petropoulou M., (2014), Influence of local and regional sources on the observed spatial and temporal variability of size resolved atmospheric aerosol mass concentrations and water-soluble species in the Athens metropolitan area, Atmospheric Environment, 97: 252–261.

Grigoratos Th., Samara C., Voutsa D., Manoli E., Kouras A., (2014), Chemical composition and mass closure of the coarse particle fraction at kerbside and urban background sites. Environmental Science and Pollution Research 21, 7708–7722 (DOI 10.1007/s11356-014-2732-z).

Grivas G., Cheristanidis S., Chaloulakou A., (2012), Elemental and organic carbon in the urban environment of Athens. Seasonal and diurnal variations and estimates of secondary organic carbon. Science of The Total Environment, 414: 535–545.

ISO/IEC EN-12341: "Ambient air. Standard gravimetric measurement method for the determination of the PM10 or PM2.5 mass concentration of suspended particulate matter".

ISO/IEC EN-14907: "Ambient air quality. Standard gravimetric measurement method for the determination of the PM2.5 mass fraction of suspended particulate matter".

Pateraki St., Asimakopoulos D.N., Bougiatioti A., Maggos Th., Vasilakos Ch., Mihalopoulos N., (2014), Assessment of $PM_{2.5}$ and PM_1 chemical profile in a multiple-impacted Mediterranean urban area: Origin, sources and meteorological dependence. Science of The Total Environment, 479–480: 210–220.

Samara C., Voutsa D, Kouras A., Eleftheriadis K., MaggosTh, Saraga D., Petrakakis M., (2013), Organic and elemental carbon associated to PM_{10} and $PM_{2.5}$ at urban sites of northern Greece. Environmental Science and Pollution Research, DOI 10.1007/s11356-013-2052-8.

Samara C., Tsitouridou R., (2000), Fine and coarse ionic aerosol components in relation to wet and dry deposition. Water, Air, and Soil Pollution, 120: 71–88.

Terzi E., Argyropoulos G., Bougatioti A., Mihalopoulos N., Nikolaou K., Samara C., (2010), Chemical composition and mass closure of ambient PM_{10} at urban sites. Atmospheric Environment, 44: 2231-2239.

Theodosi C., Grivas G., Zarmpas P., Chaloulakou A., Mihalopoulos N., (2011), Mass and chemical composition of size-segregated aerosols (PM_1,$PM_{2.5}$, PM_{10}) over

Athens, Greece: local versus regional sources. Atmospheric Chemistry and Physics, 11, 11895-11911, doi:10.5194/acp-11-11895-2011

Tsitouridou R., Voutsa, D., Kouimtzis Th., (2003), Ionic composition of PM_{10} in the area of Thessaloniki, Greece. Chemosphere, 52: 883–891.

Turpin B.J., Lim H.-J., (2001), Species contributions to $PM_{2.5}$ mass concentrations: Revisiting common assumptions for estimating organic mass. Aerosol Science and Technology, 35: 602–610.

Viana M., Chi X., Maenhaut W., Querol X., Alastuey A., Mikuska P., Vecera Z., (2006), Organic and elemental carbon concentrations in carbonaceous aerosols during summer and winter sampling campaigns in Barcelona, Spain. Atmospheric Environment, 40: 2180–2193.

Voutsa D., Samara C., Manoli E., Gounari E., Lazarou D., Tzoumaka P., (2014), Ionic composition of $PM_{2.5}$ at urban sites of northern Greece - Secondary inorganic aerosol formation. Environmental Science and Pollution Research 21, 7, 4995-5006 (DOI 10.1007/s11356-013-2445-8).

Voutsa D, Samara C., Kouimtzis Th., Ochsenkühn K., (2002), Elemental composition of airborne particulate matter in the multi-impacted urban area of Thessaloniki, Greece. Atmospheric Environment, 36(28): 4453–4462.

ANNEX I: Concentration of major ionic components

Table I Average (MV) and Standard Deviation (SD) in μg m^{-3}.

Warm	AMA/AP		AMA/NS		TMA/UT		TMA/UB		VGA/UTH	
PM_{10}	MV	SD	MV	SD	MV	SD	MV	SD	MV	SD
Na^+	0.69	0.83	0.53	0.33	0.30	0.33	0.31	0.33	0.26	0.07
NH_4^+	0.74	0.35	1.00	0.40	1.29	1.16	1.40	1.11	1.12	0.47
K^+	0.15	0.10	0.22	0.12	0.16	0.09	0.15	0.07	0.26	0.07
Mg^{2+}	0.08	0.05	0.08	0.04	0.03	0.02	0.03	0.02	0.05	0.01
Ca^{2+}	0.79	0.31	1.11	0.45	1.10	0.70	0.83	0.38	1.14	0.16
Cl^-	0.28	0.46	0.17	0.17	0.26	0.22	0.25	0.22	0.53	0.32
NO_3^-	0.73	0.50	0.74	0.39	1.08	0.98	1.40	2.20	0.46	0.38
SO_4^{2-}	3.46	1.33	5.20	2.12	4.20	2.00	4.17	1.41	5.01	1.57
Cold	**AMA/AP**		**AMA/NS**		**TMA/UT**		**TMA/UB**		**VGA/UTH**	
PM_{10}	MV	SD	MV	SD	MV	SD	MV	SD	MV	SD
Na^+	0.87	0.73	0.83	0.69	0.12	0.21	0.11	0.22	0.75	0.41
NH_4^+	0.87	0.40	2.09	1.18	1.78	1.86	2.37	1.85	3.18	1.80
K^+	0.17	0.05	0.45	0.23	0.17	0.11	0.16	0.09	2.83	1.78
Mg^{2+}	0.11	0.09	0.12	0.09	0.02	0.02	0.02	0.01	0.10	0.07
Ca^{2+}	0.60	0.53	1.36	0.86	1.95	1.25	1.07	0.69	2.05	1.37
Cl^-	0.69	0.79	0.48	0.59	0.47	0.36	0.34	0.28	0.67	0.49
NO_3^-	1.48	1.00	3.16	3.29	5.04	3.31	4.58	3.73	4.32	1.84
SO_4^{2-}	2.90	1.25	6.69	3.95	4.54	1.97	4.63	1.98	9.77	4.62
Warm	**AMA/AP**		**AMA/NS**		**TMA/UT**		**TMA/UB**		**VGA/UTH**	
$PM_{2.5}$	MV	SD	MV	SD	MV	SD	MV	SD	MV	SD
Na^+	0.09	0.10	0.25	0.25	0.10	0.09	0.12	0.07	0.15	0.05
NH_4^+	0.98	0.43	1.32	0.49	1.95	0.94	2.10	0.68	1.17	0.43
K^+	0.09	0.07	0.17	0.10	0.08	0.06	0.11	0.05	0.25	0.08
Mg^{2+}	0.02	0.01	0.04	0.02	0.02	0.01	0.02	0.01	0.02	0.01
Ca^{2+}	0.13	0.13	0.36	0.28	0.28	0.23	0.18	0.07	0.46	0.17
Cl^-	0.02	0.05	0.04	0.07	0.24	0.07	0.09	0.05	0.05	0.02
NO_3^-	0.15	0.13	0.25	0.23	0.63	1.14	0.16	0.12	0.23	0.22
SO_4^{2-}	2.57	1.03	4.57	1.72	4.07	1.58	4.56	1.35	4.32	1.37
Cold	**AMA/AP**		**AMA/NS**		**TMA/UT**		**TMA/UB**		**VGA/UTH**	
$PM_{2.5}$	MV	SD	MV	SD	MV	SD	MV	SD	MV	SD
Na^+	0.20	0.14	0.32	0.26	0.07	0.07	0.06	0.05	0.48	0.24
NH_4^+	1.00	0.52	1.22	0.54	4.08	2.95	4.25	3.17	1.65	1.14
K^+	0.12	0.04	0.27	0.16	0.14	0.07	0.13	0.07	1.92	1.10
Mg^{2+}	0.03	0.02	0.05	0.03	0.01	0.00	0.01	0.01	0.05	0.03
Ca^{2+}	0.11	0.09	0.37	0.24	0.26	0.12	0.17	0.09	0.79	0.38
Cl^-	0.05	0.13	0.15	0.23	0.41	0.23	0.18	0.15	0.46	0.57
NO_3^-	0.33	0.27	1.86	2.02	5.03	5.65	3.55	3.68	3.13	1.80
SO_4^{2-}	2.32	1.13	2.88	1.23	4.18	2.29	4.44	2.29	5.15	2.57

ANNEX II: Concentration of major and trace elements

Table II Average (MV) and Standard Deviation (SD) in ng m^{-3}.

Warm	AMA/AP		AMA/NS		TMA/UT		TMA/UB		VGA/UTH	
PM_{10}	MV	SD	MV	SD	MV	SD	MV	SD	MV	SD
Mg	116.9	54.5	88.8	50.2	298.8	139.2	154.8	122.4	118.1	36.5
Al	405.0	252.7	198.5	119.7	601.0	282.5	336.7	309.6	760.7	583.9
Si	917.2	526.9	629.6	409.2	1255	585.2	674.5	613.7	872.7	443.4
S	1210	452.3	806.6	343.6	1373	692.2	540.6	611.3	1241	233.6
Cl	202.6	255.7	193.0	254.3	75.9	118.8	57.9	80.5	136.5	104.2
K	449.4	189.7	312.6	152.3	531.0	207.5	321.1	210.7	526.2	213.9
Ca	1590	783.1	1414	1081	3447	1687	1409	950.5	1202	759.7
Ti	34.1	21.0	17.6	9.9	53.5	18.3	30.4	16.6	28.1	13.7
V	5.5	4.1	7.3	7.7	7.0	5.0	3.7	2.3	5.2	3.1
Mn	14.9	8.9	12.7	6.2	67.3	47.9	31.6	21.7	34.6	17.0
Fe	562.1	316.0	448.2	198.6	1244	474.6	529.2	237.9	944.4	531.8
Ni	6.5	5.8	5.5	4.0	9.3	7.5	5.5	4.0	7.6	2.9
Co	3.9	2.7	9.4	11.0	6.8	5.1	2.6	1.4	2.2	3.1
Cr	20.5	19.7	4.8	2.5	18.8	7.9	10.0	4.7	6.6	4.3
As	2.0	3.4	2.2	2.5	1.6	3.6	0.8	1.5	1.7	2.4
Cd	0.3	0.3	0.9	0.5	1.4	0.9	3.2	7.9	0.1	0.1
Cu	11.5	16.8	13.1	6.4	36.4	13.9	7.9	4.6	14.0	8.6
Zn	59.4	58.1	61.0	51.8	75.5	43.2	32.1	18.8	124.9	111.8
Br	54.4	22.5	32.7	12.1	52.6	18.6	47.5	14.2	55.4	15.3
Sr	4.3	3.1	8.2	6.9	12.7	6.3	8.9	3.8	9.2	5.4
Sb	10.2	7.7	3.2	2.2	5.2	2.1	5.0	2.4	1.3	1.1
Ba	18.8	15.1	8.0	7.3	15.3	5.2	11.3	2.7	-	-
Pb	9.0	7.7	10.5	6.6	20.2	19.3	11.1	10.5	22.6	16.7
Cold	**AMA/AP**		**AMA/NS**		**TMA/UT**		**TMA/UB**		**VGA/UTH**	
PM_{10}	MV	SD	MV	SD	MV	SD	MV	SD	MV	SD
Mg	134.1	123.0	158.4	124.0	136.3	54.8	84.7	43.0	117.5	58.5
Al	262.1	523.7	256.3	367.9	290.3	122.8	225.4	128.7	178.3	88.6
Si	584.9	1156	555.8	823.0	709.1	334.0	518.7	322.2	390.8	238.5
S	905.5	438.8	1346	805.8	1124	458.5	1054	415.4	2189	989.1
Cl	462.6	500.9	572.6	703.9	251.7	205.7	151.7	140.5	564.4	554.4
K	361.8	291.4	607.6	329.8	582.3	245.6	551.4	215.3	2038	1480
Ca	980.2	1059	1554	1389	4540	2565	1981	1144	2630	2273
Ti	24.1	45.6	31.7	42.3	46.1	15.4	26.9	12.5	19.9	13.9
V	5.2	2.9	18.2	16.9	6.9	4.2	6.0	3.4	10.8	9.6
Mn	11.9	9.6	19.2	13.9	44.5	25.2	22.1	12.7	45.6	27.8
Fe	386.4	475.4	751.2	726.3	1319	439.8	452.2	233.6	1109	855.4
Ni	4.3	2.5	9.3	8.9	10.2	5.9	6.8	4.4	9.2	5.6
Co	9.0	8.0	2.4	3.1	5.9	3.8	2.9	1.9	1.7	1.3
Cr	7.9	7.9	9.3	14.3	18.2	5.0	7.8	3.7	20.6	22.4

As	2.8	7.9	0.5	0.6	2.1	2.3	1.1	1.8	8.3	5.3
Cd	0.1	0.1	0.4	0.3	0.4	0.4	0.2	0.2	0.3	0.2
Cu	10.8	6.5	23.2	18.3	42.4	14.9	10.7	7.6	31.1	14.7
Zn	24.8	22.7	51.4	39.1	105.9	73.7	61.3	59.6	227.3	256.8
Br	44.3	20.9	76.5	50.3	51.3	16.3	62.9	51.0	87.8	33.9
Sr	3.5	6.8	14.3	15.8	9.7	4.6	7.6	2.6	1.7	2.6
Sb	3.5	2.2	4.2	6.8	5.4	2.6	3.8	1.0	4.1	3.3
Ba	21.3	19.6	19.4	19.0	13.3	3.7	11.1	0.6	-	-
Pb	7.3	4.0	18.4	12.7	19.2	9.2	12.8	8.1	44.5	32.6
Warm	**AMA/AP**		**AMA/NS**		**TMA/UT**		**TMA/UB**		**VGA/UTH**	
$PM_{2.5}$	**MV**	**SD**	**MV**	**SD**	**MV**	**SD**	**MV**	**SD**	**MV**	**SD**
Mg	28.6	16.6	35.2	19.7	62.2	52.7	37.0	24.6	66.8	21.1
Al	74.2	42.4	64.9	35.3	119.2	76.5	78.9	70.3	157.4	76.2
Si	166.5	98.3	183.8	130.4	221.3	167.8	129.9	142.4	378.9	183.7
S	1086	431.7	984.2	332.9	1125	575.1	771.4	727.9	1183	355.7
Cl	13.9	15.9	11.9	11.0	6.4	14.0	0.9	1.2	16.6	10.7
K	209.9	127.0	190.4	129.0	238.5	123.8	203.8	126.7	333.8	138.9
Ca	224.9	102.7	413.4	353.1	486.7	524.9	173.6	142.0	858.2	404.1
Ti	5.8	3.8	6.9	4.8	13.5	5.0	10.0	3.1	13.3	6.4
V	4.4	2.7	7.6	7.5	4.8	3.3	3.7	1.7	4.8	3.0
Mn	2.9	2.6	5.1	4.5	16.5	11.0	9.1	5.1	19.3	10.1
Fe	120.7	56.8	163.8	99.6	275.5	130.5	122.6	53.3	374.5	214.9
Ni	2.6	1.9	3.7	3.0	3.6	2.3	3.3	1.8	3.8	2.0
Co	2.2	1.3	1.2	1.2	3.1	1.7	2.3	1.1	1.6	2.4
Cr	1.1	1.2	6.0	11.5	6.6	3.4	4.6	1.8	2.2	1.3
As	2.2	3.6	2.1	2.4	1.5	6.0	0.7	2.4	0.5	0.9
Cd	0.3	0.2	0.7	0.6	1.5	0.7	0.9	0.9	0.1	0.1
Cu	2.8	2.4	9.1	4.1	10.3	4.3	3.6	2.1	8.5	5.6
Zn	33.4	33.4	48.5	45.5	48.6	41.3	26.4	16.4	90.4	88.2
Br	33.3	14.0	25.6	9.4	42.2	15.6	41.8	10.5	45.7	11.9
Sr	2.1	2.0	3.2	2.9	5.8	2.7	5.8	3.4	6.5	5.6
Sb	5.5	4.2	2.0	1.7	4.2	1.9	3.5	0.0	0.8	0.7
Ba	8.3	6.6	5.6	5.1	11.5	2.2	10.8	0.0	-	-
Pb	4.9	4.5	12.1	7.7	16.5	29.2	9.7	10.8	21.5	16.5
Cold	**AMA/AP**		**AMA/NS**		**TMA/UT**		**TMA/UB**		**VGA/UTH**	
$PM_{2.5}$	**MV**	**SD**	**MV**	**SD**	**MV**	**SD**	**MV**	**SD**	**MV**	**SD**
Mg	45.3	40.4	45.6	39.5	18.7	8.2	16.3	6.3	21.4	24.2
Al	78.9	157.5	54.0	102.5	48.7	21.9	41.4	19.4	42.2	31.4
Si	151.2	325.5	2.3	4.5	80.2	63.1	61.8	53.4	92.2	73.1
S	803.9	349.4	601.0	314.0	815.9	500.0	863.9	421.7	1131	385.0
Cl	37.1	64.3	79.5	134.4	45.2	48.1	51.1	63.9	352.7	413.7
K	206.6	95.8	235.9	160.0	345.6	173.3	349.3	149.9	1184	921.8
Ca	152.6	160.0	336.9	260.6	380.8	348.9	174.2	145.7	636.7	533.4

Ti	6.1	10.2	6.8	7.5	11.7	2.4	9.6	2.2	3.1	3.3
V	4.8	2.6	10.5	7.9	6.8	3.5	5.4	3.3	5.8	4.6
Mn	4.8	4.2	4.1	3.6	11.1	5.0	6.9	3.9	18.2	9.4
Fe	107.5	105.6	133.1	90.7	169.1	77.0	95.6	46.3	270.7	166.6
Ni	2.6	1.5	3.7	2.5	4.6	2.7	3.1	2.1	3.9	2.3
Co	5.4	3.7	1.5	1.5	2.8	1.4	2.4	1.1	0.9	0.5
Cr	2.2	2.3	2.3	1.5	6.4	4.1	5.5	2.6	1.8	1.6
As	2.6	7.8	0.4	0.3	0.7	1.4	0.6	0.9	5.1	3.3
Cd	0.1	0.1	0.1	0.1	0.2	0.2	0.2	0.2	0.0	0.0
Cu	2.5	2.6	7.0	5.4	9.2	8.4	4.5	5.1	13.3	7.7
Zn	15.6	13.1	25.0	24.5	56.8	40.2	40.0	38.0	127.3	121.4
Br	26.2	17.9	33.2	21.5	54.7	59.6	46.9	40.7	43.2	21.7
Sr	0.7	1.4	5.6	5.0	7.7	4.7	6.3	3.8	4.2	4.8
Sb	1.4	1.2	1.2	1.0	5.4	3.6	4.4	2.9	0.4	0.4
Ba	12.9	10.9	10.4	9.9	12.8	3.4	11.4	1.9	-	-
Pb	2.8	3.0	10.1	9.2	13.1	7.8	10.8	8.4	26.0	16.7